

Molecular Mechanisms of Liver Carcinogenesis in the Mdr2-Knockout Mice

Mark Katzenellenbogen,¹ Lina Mizrahi,¹ Orit Pappo,² Naama Klopstock,¹ Devorah Olam,¹ Jasmine Jacob-Hirsch,³ Ninette Amariglio,³ Gideon Rechavi,³ Eytan Domany,⁴ Eithan Galun,¹ and Daniel Goldenberg¹

¹Goldyne Savad Institute of Gene Therapy and ²Department of Pathology, Hadassah-Hebrew University Medical Center, Jerusalem, Israel; ³Institute of Hematology and Sheba Cancer Research Center, Sackler School of Medicine, Tel Aviv University, Tel Hashomer, Israel; and ⁴Department of Physics of Complex Systems, Weizmann Institute of Science, Rehovot, Israel

Abstract

Mouse models of hepatocellular carcinoma (HCC) simulate specific subgroups of human HCC. We investigated hepatocarcinogenesis in Mdr2-knockout (Mdr2-KO) mice, a model of inflammation-associated HCC, using gene expression profiling and immunohistochemical analyses. Gene expression profiling showed that although Mdr2-KO mice differ from other published murine HCC models, they share several important deregulated pathways and many coordinately differentially expressed genes with human HCC data sets. Analysis of genome positions of differentially expressed genes in liver tumors revealed a prolonged region of down-regulated genes on murine chromosome 8 in three of the six analyzed tumor samples. This region is syntenic to human chromosomal regions that are frequently deleted in human HCC and harbor multiple tumor suppressor genes. Real-time reverse transcription-PCR analysis of 16 tumor samples confirmed down-regulation of several tumor suppressors in most tumors. We show that in the aged Mdr2-KO mice, cyclin D1 nuclear level is increased in dysplastic hepatocytes that do not form nodules; however, it is decreased in most dysplastic nodules and in liver tumors. We found that this decrease is mostly at the protein, rather than the mRNA, level.

These findings raise the question on the role of cyclin D1 at early stages of hepatocarcinogenesis in the Mdr2-KO HCC model. Furthermore, we show that most liver tumors in Mdr2-KO mice were characterized by the absence of β -catenin activation. In conclusion, the Mdr2-KO mouse may serve as a model for β -catenin-negative subgroup of human HCCs characterized by low nuclear cyclin D1 levels in tumor cells and by down-regulation of multiple tumor suppressor genes. (Mol Cancer Res 2007;5(11):1159–70)

Introduction

Human hepatocellular carcinoma (HCC) is one of the major health care burdens, the molecular pathogenesis of which is still not well understood. Mouse models of HCC have been widely used to study the molecular mechanisms of the disease and to test new therapeutic approaches. Comparison of global expression patterns of orthologous genes in human and murine HCCs showed that certain mouse HCC models closely reproduce specific subgroups of human HCCs (1, 2). Mdr2-knockout (Mdr2-KO) mice represent a model of inflammation-associated HCC (3). They lack the liver-specific P-glycoprotein responsible for phosphatidylcholine transport across the bile canalicular membrane. The absence of phospholipids from bile results in bile regurgitation into the portal tracts (4), causing portal inflammation and fibrosis that mimic human progressive familial intrahepatic cholestasis (5). Liver inflammation and toxicity induced by bile salts in Mdr2-KO mice lead to the development of hepatocyte dysplasia, and by 16 months of age, virtually 100% of Mdr2-KO mice show liver tumors. It was previously found that both tumor necrosis factor α and nuclear factor κ B are elevated in inflamed portal tracts of Mdr2-KO mice, and that reduction of tumor necrosis factor- α levels or nuclear factor κ B inactivation prevented tumor development, providing a rational link between inflammation and tumorigenesis in this HCC model (6).

We have recently shown that the precancerous stages of liver disease in the Mdr2-KO mice are characterized by induction of many oncogenes, on one hand, and by multiple protective mechanisms, including up-regulation of many anti-inflammatory and antioxidant genes, on the other hand (7). We have also revealed an age-dependent progressive deregulation of genes that control lipid metabolism; this effect is probably responsible for the

Received 4/12/07; revised 6/21/07; accepted 7/19/07.

Grant support: Salzberg Foundation and Kamea Scientific Foundation of the Israeli Government (D. Goldenberg); Blum Foundation, Greenspoon Foundation, Horwitz Foundation, and Israeli Science Ministry grant for support of the Gene Therapy Strategic Center (E. Galun); Horwitz Foundation through The Center for Complexity Science and a Jewish National fund grant in memory of Arthur and Ludmila Zuker (M. Katzenellenbogen).

The costs of publication of this article were defrayed in part by the payment of page charges. This article must therefore be hereby marked *advertisement* in accordance with 18 U.S.C. Section 1734 solely to indicate this fact.

Note: Supplementary data for this article are available at Molecular Cancer Research Online (<http://mcr.aacrjournals.org/>).

E. Galun holds the Sam and Ellie Fishman Chair in Gene Therapy. E. Domany is the incumbent of the Henry J. Leir Professorial Chair.

Requests for reprints: Daniel Goldenberg, Goldyne Savad Institute of Gene Therapy, Hadassah-Hebrew University Medical Center, Kiryat Hadassah, P.O. Box 12000, Jerusalem 91120, Israel. Phone: 972-2-677-8108; Fax: 972-2-643-0982. E-mail: goldenberg@hadassah.org.il

Copyright © 2007 American Association for Cancer Research.

doi:10.1158/1541-7786.MCR-07-0172

frequent appearance of steatotic dysplastic nodules in the livers of Mdr2-KO mice at 12 months of age. Here, we continue our study on the molecular mechanisms of hepatocarcinogenesis in Mdr2-KO mice by characterizing the cancerous stage of liver disease in this HCC model. We compare the results of the global gene expression profiling of tumorous and nontumorous liver tissues from Mdr2-KO mice at 16 months of age with other published data on global expression profiling of mouse HCC models and human HCC samples (1). We determine the dynamic changes in Mdr2-KO livers between mice at 12 and 16 months of age and the essential differences between tumorous, nontumorous, and control liver tissues of Mdr2-KO mice at 16 months of age. The most important microarray findings were confirmed by real-time reverse transcription-PCR (RT-PCR) and by immunohistochemistry on the expanded set of Mdr2-KO liver tumors. We show that the Mdr2-KO HCC model shares many deregulated HCC-associated genes and pathways with human HCC and is more similar to human HCC cases characterized by better survival (8). We show that Mdr2-KO tumors are characterized by down-regulation of transcripts of multiple tumor suppressor genes and by the absence of β -catenin activation. We also show an intriguing pattern of nuclear staining of cyclin D1 in hepatocytes, which raises a question about the role of this well-known oncogene in hepatocarcinogenesis in the Mdr2-KO HCC model.

Results

Liver Tumor Development

We have previously described that livers of Mdr2-KO mice at 12 months of age were characterized by disrupted lobular structure and appearance of dysplastic nodules, some of them being steatotic (7). The number and size of visible liver tumors in Mdr2-KO mice increased gradually with age. At 16 months of age, almost all Mdr2-KO mice had at least one tumor with a diameter of at least 0.5 cm. In rare cases, tumors could also be found in mice between the ages of 9 and 12 months.

The number of steatotic degenerated hepatocytes also increased with age, and a significant proportion of tumors were steatotic as well. We have analyzed 21 tumor tissue samples from 10 Mdr2-KO males at 16 months of age: for 11 tumors, both formalin-fixed and frozen tissue samples were analyzed; for additional 5 tumors, only formalin-fixed tissue samples were accessible; and for another 5 tumor samples, only frozen tissue samples were accessible (Table 1). Most tumors were well-differentiated HCC as determined by their aberrant growth patterns (thick trabeculae, acinar, and solid growth) and absence of portal tracts. Hepatocyte variability in nuclear size was similar to that in surrounding nontumorous liver tissue. Some tumors were also classified as moderately differentiated HCC, based on predominantly trabecular and solid growth patterns, prominent nucleoli observed in >50% of hepatocytes, and marked hepatocyte pleomorphism compared with surrounding nontumorous liver tissue. Number of mitoses observed in tumors varied from 5 to 56 per 50 high-power fields (Table 1).

Common Characterization of Gene Expression in Tumors

The liver RNA samples from six Mdr2-KO tumors, six nontumorous liver tissues (four matched and two unmatched), and three control heterozygous mice at 16 months of age were

subjected to gene expression profiling using the genome-scale Affymetrix Mouse Genome 430 2.0 Array. Cluster analysis (9, 10) of the expression profiling data revealed increased heterogeneity of samples as follows: tumorous > nontumorous > heterozygous controls (Fig. 1). This analysis enabled separation of heterozygous samples from Mdr2-KO nontumorous tissues in the space of all the involved genes (these two groups form two fairly distinct clusters). On the other hand, the tumors exhibited high variability and differed from each other. A similar separation of tumor samples was obtained using the clusters of genes with tendency to down-regulation in tumors (Supplementary Fig. S1). These gene clusters separated tumors from both nontumorous tissues and the heterozygous controls.

The clustering results were in accord with the results of supervised analysis (Fig. 2) showing that (a) genes down-regulated in tumors were more statistically significant for separating tumors from nontumorous liver samples than genes up-regulated in tumors, and (b) most genes differentially expressed between nontumorous tissues and heterozygous controls were also differentially expressed between tumors and heterozygous controls, but not vice versa.

Functional Analysis of Differentially Expressed Genes

A substantial fraction of genes differentially expressed in nontumorous tissues of Mdr2-KO mice, when compared with Mdr2-heterozygotes at age 16 months (Supplementary Table S1), was also differentially expressed in Mdr2-KO tissues when compared with Mdr2-heterozygotes at 3 and 12 months of age (7). The common fraction of genes up-regulated both at 12 and 16 months of age was enriched with "cell adhesion", "cell communication", and "defense response" genes and contained many potential oncogenes discussed previously (7). The functional study of differentially expressed genes in 16-month-old mice using pathway-oriented and Gene Ontology enrichment analyses revealed progressive down-regulation of liver-specific genes in tumors and Mdr2-KO nontumorous liver tissues compared with heterozygous controls. The most significantly enriched fractions among genes up-regulated in tumors compared with heterozygous tissues were genes related to such Gene Ontology biological processes as "cell proliferation", "cytoskeleton organization and biogenesis", and "cell adhesion". The latter category was also the most enriched among the genes up-regulated in Mdr2-KO nontumorous tissues compared with heterozygotes. Remarkably, the majority of the discovered cell cycle-related genes up-regulated in tumorous and nontumorous Mdr2-KO samples compared with heterozygous controls were involved in the advanced stages of mitosis. Several transcriptional targets of β -catenin, including specific markers of its activation (11, 12), were down-regulated in most Mdr2-KO tumors. Analysis of the known transcriptional targets of other oncogenic pathways showed no convincing evidence of activation in Mdr2-KO tumors of p53, Rb, or Myc regulatory pathways. Several genes that were previously shown to correlate with p53 staining in human HCC (13) were coordinately differentially regulated between tumor samples and heterozygotes in some Mdr2-KO tumor samples. However, immunohistochemical staining of 16 tested Mdr2-KO liver tumors (listed in Table 1) with anti-p53 antibody did not reveal p53 accumulation in any of them (not shown).

TABLE 1. Characterization of Liver Tumors of 16-Month-Old Mdr2-KO Mice

Tumor No.	Tumor Diameter (cm)	Tumor Grade	Mitoses per 50 HPF	Gene Expression Relative to the Matched Nontumorous Liver Tissue*								
				Cyclin D1	Cdh1	Cdkn1b	Dleu2	Lats1	Mxi1	Plagl1	Rbl2	Ubd
49T1	>1.3	Well †	5		Down						Down	
84T1	>1.3	Well	7		Down		Down				Down	Down
85T1 ‡	0.5-0.7	Well/mod.	4									
85T2 †	0.5-0.7				Down						Down	
85T3 †	0.5-0.7											
93T1	1.1-1.3	Well	18	Down	Down							
93T2 †	0.5-0.7				Down	Down						Up
94T1 ‡	0.5-0.7	Well	7									
96T1	>1.3	Well	9									
96T2 †	0.5-0.7				Down		Down				Down	Up
704T1 ‡	0.5-0.7	Well/mod.	56									
704T2 ‡	0.5-0.7	Well/mod.	25									
704T3 ‡	0.5-0.7	Well	19									
705T1	>1.3	Mod.	5			Down	Down	Down	Down	Down	Down	Up
705T2	1.1-1.3	Mod.	15	Down	Down		Down	Down		Down	Down	Up
706T1	>1.3	Well	6	Down	Down					Down		Up
706T2	1.1-1.3	Well	25									Up
706T3	0.8-1.0	Well	10									
707T1	>1.3	Well	36	Down			Down				Down	Up
707T2	0.8-1.0	Well	6									
707T3 †	0.5-0.7				Down		Down		Down	Down	Down	Up

NOTE: Tumors that were analyzed by gene expression profiling are shown in boldface.

Abbreviation: HPF, high-power field ($\times 200$).

*Results of the real-time RT-PCR. Only genes down-regulated or up-regulated at least 2-fold are shown.

†Tumors represented by frozen samples only.

‡Tumors represented by histologic samples only.

Chromosomal Analysis

Chromosomal aberrations are frequent in liver cancer (14) and can be a reason for the variability of gene expression profiles in tumors. Recently, it was shown that an approximate

evaluation of DNA ploidy of large chromosomal regions may be deduced from the gene expression profile based on the suggestion that a deleted (or an amplified) region has a tendency to decrease (or increase) the average expression levels

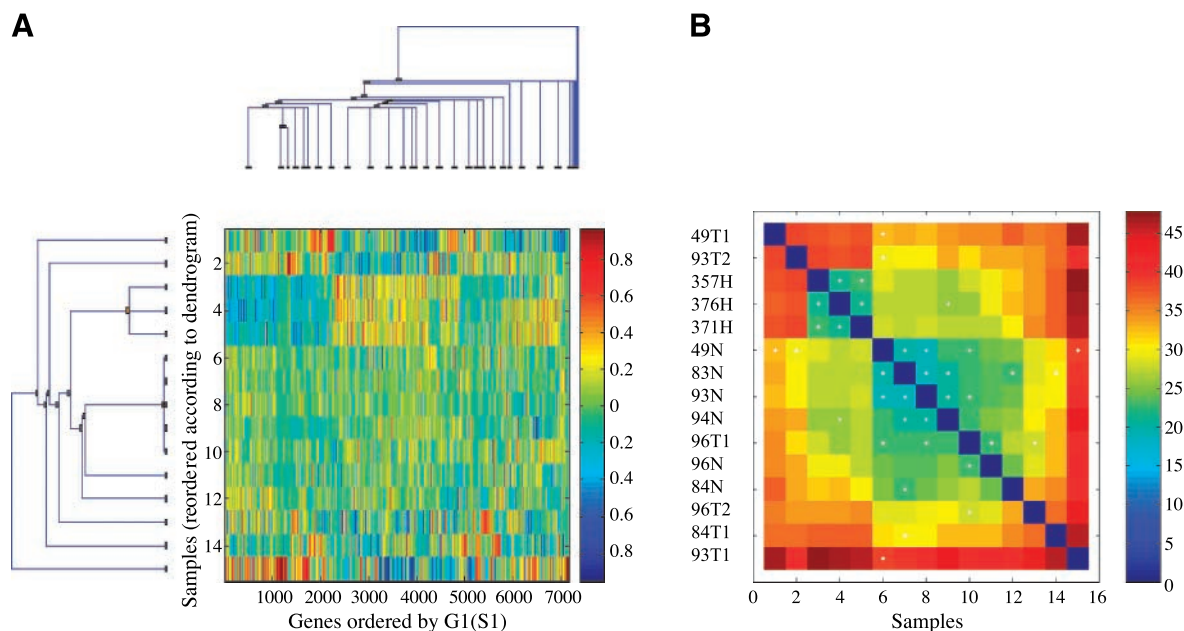


FIGURE 1. Two-dimensional clustering of gene expression data. The Mdr2-KO data set had been preprocessed by filtering of the valid Affymetrix probes with a SD filter. The 7,167 probes possessing SD for log₂ transformed values higher than 0.3 in all samples were submitted to SPC algorithm incorporated into CTWC tool. The samples include six Mdr2-KO tumorous samples (marked T), six Mdr2-KO nontumorous samples (marked N), and three heterozygous control samples (marked H). **A.** The color-coded expression matrix with aligned dendrograms of samples (*left*) and genes (*above*). The height of dendrogram branches represents the sensitivity variable (temperature) in SPC clustering algorithm. **B.** The color-coded matrix of the standardized Euclidean distances between the analyzed samples. The order of samples in **A** and **B** is identical.

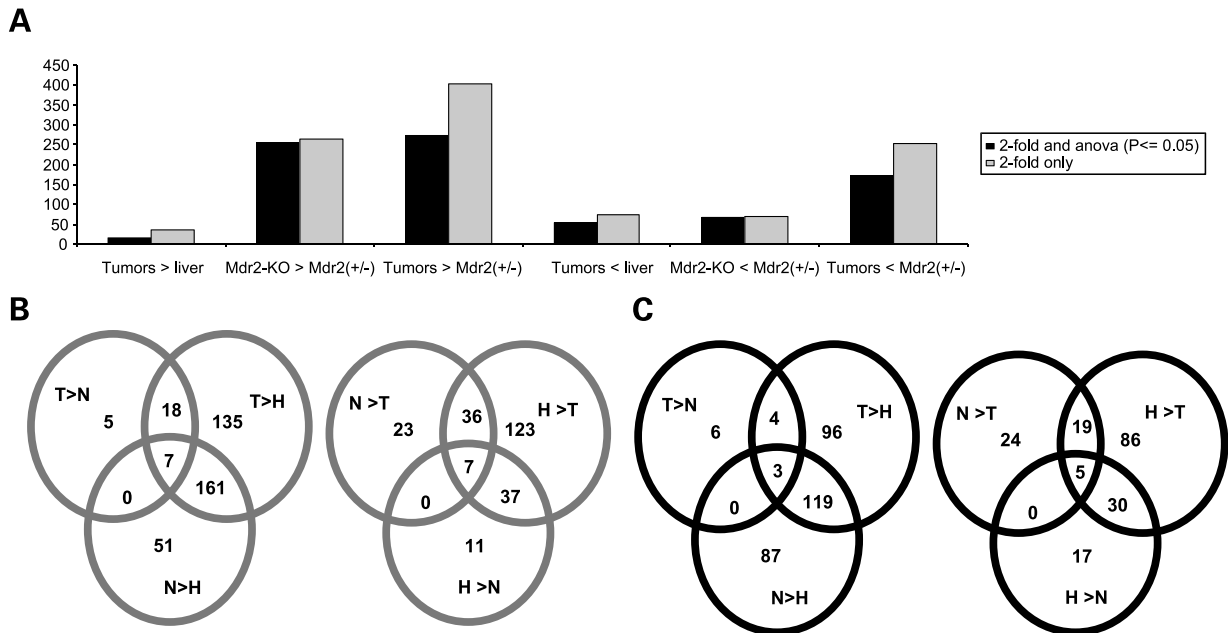


FIGURE 2. The supervised analysis of differential expression. **A.** Number of genes differentially expressed by 2-fold between the experimental groups depicted at X-axis. Data for the 2-fold changes in expression average of \log_2 -transformed values and for the 2-fold changes that were also significant in ANOVA statistical test are shown with gray and black columns, respectively. **B** and **C.** Venn diagrams showing the cross sections between the gene groups: 2-fold changes (**B**); 2-fold changes statistically validated by ANOVA test (**C**). T, tumorous; N, nontumorous; H, heterozygous liver RNA samples.

(15). Analysis of genome position–specific deviations of average gene expression in our data revealed multiple areas of up-regulation and down-regulation in tumor samples, including the longest common region of down-regulation, which was localized on chromosome 8 (Fig. 3) and found in three of the six tested tumors. Calculation of the approximate boundaries of this down-regulated (“presumed deleted”) region enabled us to map its syntenic regions in the human genome. The presumed deleted region in mice was syntenic to human chromosomal areas known to be frequently deleted in HCC: 4q2, 8p2, 16q1, and 16q2 (14, 16). These regions, both in mice and in humans, contain several genes whose loss of heterozygosity, mutations, or down-regulation was shown to be associated with HCC and other types of cancer: *Pdgfr1* (17, 18), *Vps37a* (19), *Wwox* (20), *Cdh1* (21), *Rbl2* (22), and *Cbfa2t3* (23). We confirmed reduction of copy numbers of the chromosomal region containing the *Cdh1* gene (or its loss) in all three tumor samples for which this deletion was presumed by semiquantitative PCR (Supplementary Fig. S2).

Comparison with Published Data

Gene expression patterns of tumorous and nontumorous liver tissue samples of Mdr2-KO mice were compared with those of previously published murine HCC models. For this purpose, the Affymetrix expression data set of the Mdr2-KO model was converted into a format comparable to that of two-color spotted arrays (see Materials and Methods). Hierarchical cluster analysis of the joint data set containing data of Mdr2-KO and other murine HCC models, filtered by variance criteria, enabled separation of all murine HCC models into three large clusters: cluster A, similar to human HCC with “poor survival”; cluster B, similar to human HCC with “better

survival”; and a cluster having limited relevance to human HCC, in full accordance with previously published results (1). Cluster B comprised E2f1, Myc, and Myc/E2f1 models, as well as the Mdr2-KO subcluster (Fig. 4).

Ordering the samples belonging to both cluster A and cluster B, according to their similarity in the space of the 500 most variable genes with the help of the SPIN application (24), resulted in a marginal position of Myc/transforming growth factor α and DENA model samples (cluster A) and dispersion of most Mdr2-KO samples among the samples of cluster B (Supplementary Fig. S3). Remarkably, Mdr2-KO samples were ordered in a way that could be related to tumor progression: the nontumorous samples were the most distant from the cluster A end, and the two samples expressing α -feto protein, M55T and M56T, were interspersed with the marginal cluster A samples.

Analysis of the distances between average expression profiles of different models showed the proximity of Mdr2-KO samples to E2F1 and Myc/E2f1 models (Supplementary Fig. S4A). The similarity with the E2F1 model was higher for Mdr2-KO nontumorous tissues samples, mostly on account of a relatively low number of differentially expressed genes obtained from both of these models. There was no significant up-regulation of E2F1-induced genes in the Mdr2-KO model. The Acox1 model also shared substantial similarity to Mdr2-KO tumors.

The Mdr2-KO gene expression data set was also compared with published human HCC data set (8). In full agreement with the above-mentioned results of comparison with murine HCC models (1), again we see that Mdr2-KO samples (both tumorous and nontumorous) are more similar to human HCC samples with better survival (cluster B in Fig. 4B and Supplementary

Fig. S4B) than to human samples with poor survival (cluster A in Fig. 4B). The set of genes that were down-regulated in Mdr2-KO tumorous versus nontumorous samples, and also in the human HCC versus normal samples, was enriched with metabolic genes, especially the genes involved in the metabolism of amino acids. The common set of up-regulated genes was enriched with genes classified as “cell cycle,” “cell adhesion,” and “extracellular matrix” genes.

A significant number of HCC-associated genes were found to be coordinately deregulated in Mdr2-KO mice and in published human HCC data sets (Supplementary Table S1). The most prominent among them being up-regulated—*Axl*, *Cbr3*, *Cd36*, *Lgals1*, *Lgals3*, *Jun*, and *Ubd*; down-regulated—*Ahcy*, *Cbs*, *Gnmt* (three genes encoding enzymes that control *S*-adenosylmethionine catabolism), *C6*, *C8a*, *C8b* (encoding complement components), and cytochrome *P450* genes *Cyp1a2*, *Cyp2e1*, *Cyp4v3*, *Cyp8b1* (8, 25-29). Overexpression of the *Ubd* protein may cause chromosomal instability (30). We confirmed the up-regulation of its transcript in Mdr2-KO livers by real-time RT-PCR: *Ubd* was highly up-regulated in nontumorous liver tissues (6- to 23-fold compared with Mdr2-

heterozygotes) and progressively up-regulated in most tumors (Table 1 and Supplementary Tables S2 and S3).

Down-Regulation of mRNA Level of Multiple Tumor Suppressor Genes in Tumorous Tissues of Mdr2-KO Mice

Gene expression profiling revealed down-regulation of multiple tumor suppressor genes in the tumorous tissues of Mdr2-KO mice compared with their matched nontumorous samples. Twenty-six genes annotated as “tumor suppressors” were down-regulated in at least one of the six tested tumorous RNA samples; 12 among them were down-regulated in at least two tumors and 8 were down-regulated in at least three tumors. We carried out real-time RT-PCR analysis of seven genes from the latter set on 16 tumorous RNA samples, including those 6 samples subjected to gene expression profiling. This analysis revealed that four genes (*Cdh1*, *Dleu2*, *Plagl1*, and *Rbl2*) were down-regulated each in at least 6 tumors (Table 1). Genes *Cdh1* and *Rbl2* were mapped inside the presumed deleted region on murine chromosome 8 (discussed above). Among the 16 tested tumors, 11 had down-regulation of at least two tumor

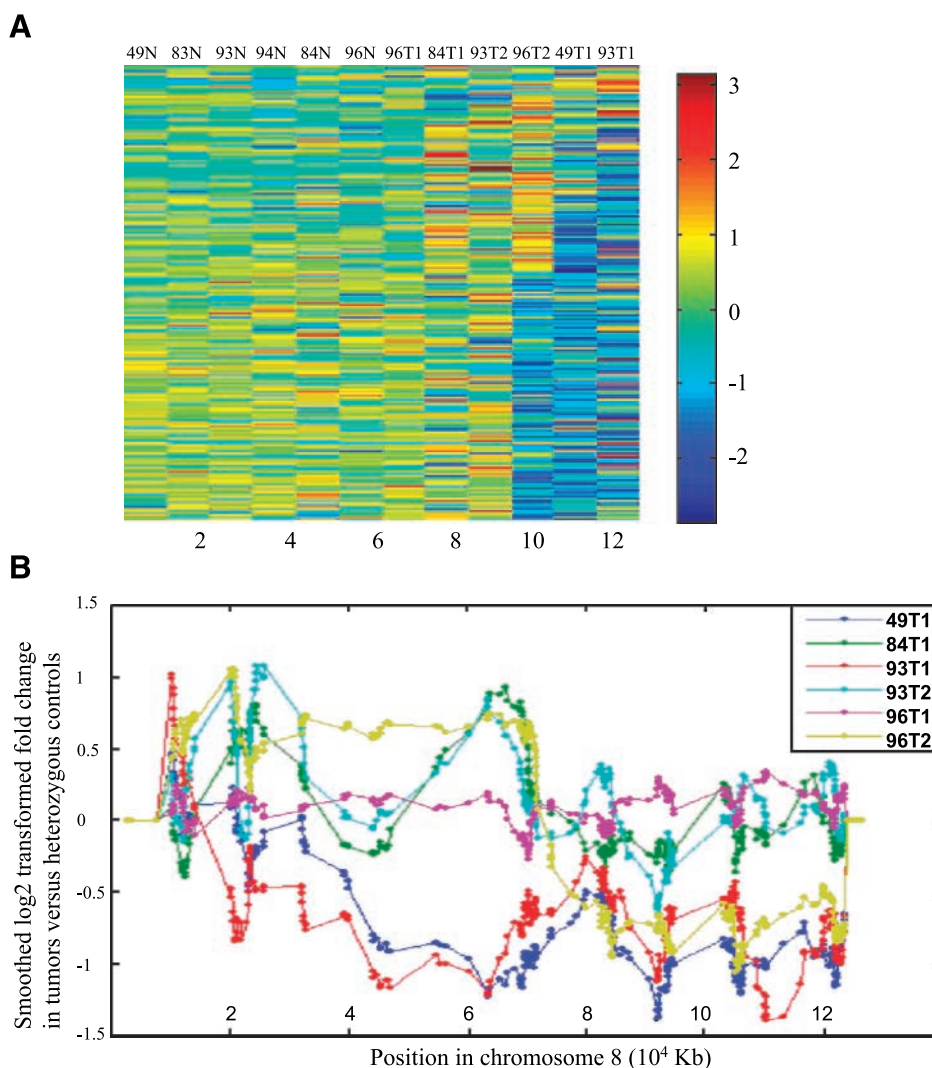


FIGURE 3. Chromosomal position-associated changes in gene expression profiles in chromosome 8. **A.** The color-coded matrix of differential expression of 306 relevant chromosome 8 genes (details in Materials and Methods) between all Mdr2-KO samples and their heterozygous controls. The genes are ordered according to their position in chromosome 8. **B.** The smoothed differential expression of genes in chromosome 8 plotted against their chromosomal positions. The smoothed differential expression was calculated as differential expression of neighboring genes between tumors and matched nontumorous liver tissues of Mdr2-KO mice (for details, see Materials and Methods).

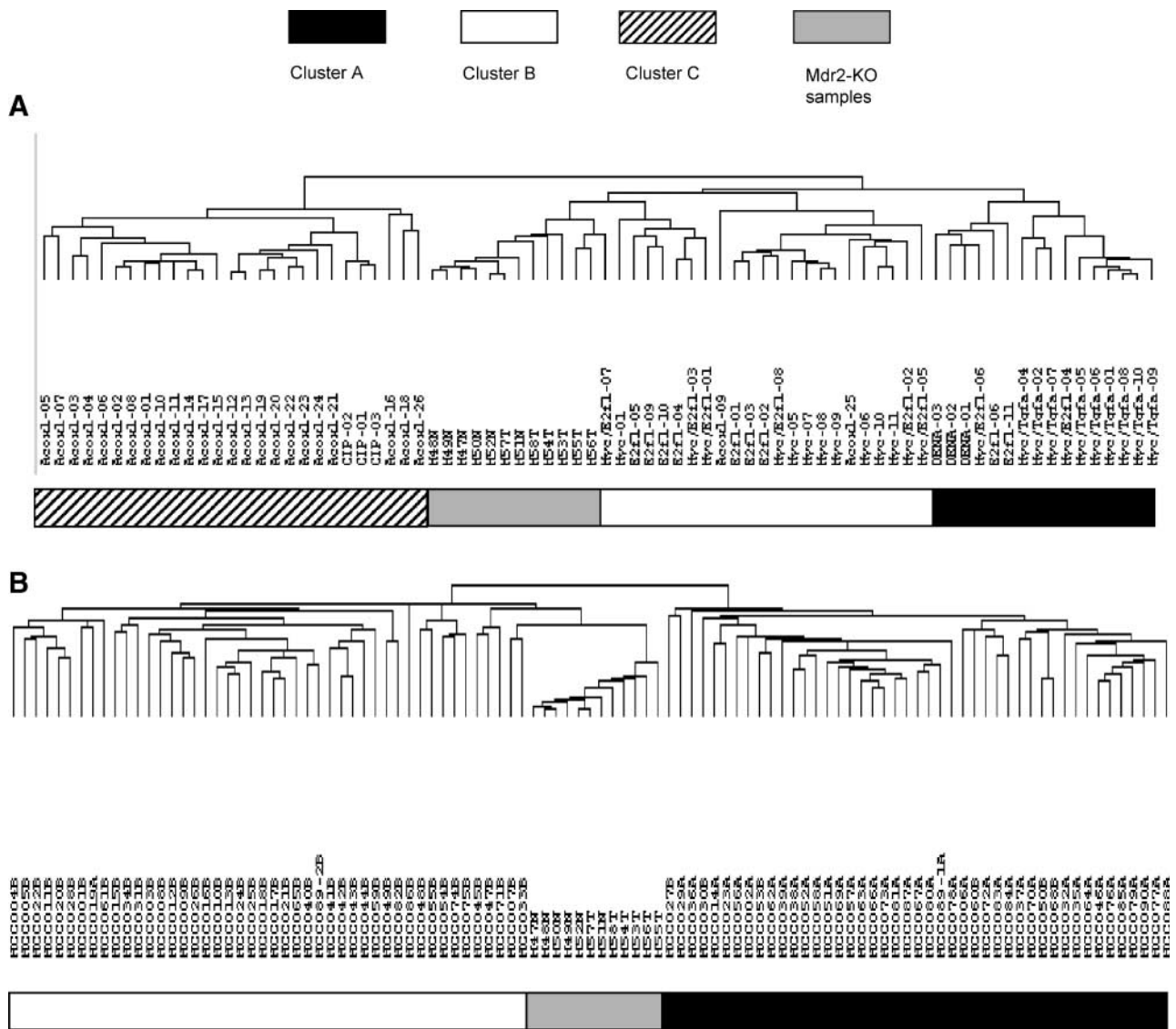


FIGURE 4. The combined clustering of gene expression data of the Mdr2-KO model with data of other murine models (A) and human HCC expression data (B). The Mdr2-KO expression data were preprocessed as described in Materials and Methods and submitted to coclustering with published murine and human expression data sets in the space of SD filtered genes with valid expression values in both compared data sets. Black, cluster A (poorer survival); white, cluster B (better survival); striped, cluster C (limited relevance to human HCC); gray, Mdr2-KO.

suppressor genes, 7 had down-regulation of at least three tumor suppressor genes, and 4 tumors had down-regulation of at least four tumor suppressor genes. Only 5 tumors exhibited no down-regulation of any of the seven tested tumor suppressor genes.

Cyclin D1 Nuclear Level Is Decreased in Hepatocytes of Tumors and Most Dysplastic Nodules in Mdr2-KO Mice

We have previously shown that during the precancerous stage, cyclin D1 is overexpressed in the livers of Mdr2-KO mice both at the mRNA (Affymetrix array) and protein (Western blot) levels (7). In the current work, we studied the cellular and cytoplasmic or nuclear localization of cyclin D1 by immunohistochemistry. High levels of nuclear cyclin D1 were found in hepatocytes of Mdr2-KO in all lobular zones during the precancerous stage at all tested ages: 3, 6, 9, and 12 months

(data for 3 and 12 months of age are presented in Fig. 5A). In the appropriate heterozygous controls, nuclear cyclin D1 staining has been observed only in a small fraction of hepatocytes in zone 2 (Fig. 5A, bottom row). The strongest nuclear cyclin D1 staining has been found in dysplastic hepatocytes that do not produce nodules, both in the cases of large-cell and small-cell dysplasia. After 9 months of age, dysplastic nodules appeared in the livers of Mdr2-KO mice. Most of these nodules were characterized by a significant decrease of nuclear cyclin D1 level in hepatocytes (Fig. 5B). Similarly, a significant decrease of nuclear cyclin D1 level was observed in all tested liver carcinomas of Mdr2-KO mice (more than 30 tumors in more than 20 animals were screened; typical example is shown in Fig. 5C). Average inclusion of bromodeoxyuridine (BrdUrd) in liver tumors was ~3-fold

higher than that in matched nontumorous regions (Fig. 5C and D), and the number of BrdUrd-positive hepatocytes directly correlated with the number of cyclin D1-negative hepatocyte nuclei (Fig. 5D), showing a higher proliferation rate of tumors with decreased nuclear cyclin D1 level. Global gene expression profiling revealed that cyclin D1 mRNA levels in nontumorous tissues of Mdr2-KO mice were ~4-fold higher than those in heterozygous controls, and remained high, although variable, in most tumorous samples. Only in one sample, D93T1, the cyclin D1 mRNA level was down-regulated compared with the matched nontumorous sample. Real-time RT-PCR of 16 tumorous RNA samples (including 6 that were subjected to Affymetrix arrays) showed down-regulation of cyclin D1 mRNA level in four samples only (Table 1). Thus, down-regulation of cyclin D1 in most liver tumors of Mdr2-KO mice takes place at the protein, rather than the mRNA, level.

Activation of the Wnt signaling is known to induce cyclin D1 expression. Gene expression profiling of six HCC tumors revealed a tendency toward down-regulation of the Wnt signaling in most of these tumors (see above). To confirm these findings and to test a correlation between cyclin D1 and β -catenin localization, we carried out β -catenin immunohistochemistry. All tested HCC tumors of Mdr2-KO mice at 16 months of age were characterized by decreased membranous staining and absence of cytoplasmic or nuclear β -catenin staining. Rare foci with high cytoplasmic β -catenin level and scattered hepatocytes with high nuclear β -catenin level were found preferentially in nontumorous liver regions (Supplementary Fig. S5, *top row*). Overall, there was no correlation between nuclear cyclin D1 level and nuclear or cytoplasmic β -catenin level; in some cases, an inverse correlation was observed (Supplementary Fig. S5). Immunohistochemistry of E-cadherin in 16-month-old Mdr2-KO mice confirmed its expression profiling data obtained by microarrays: increased expression in nontumorous tissues and decreased expression in most tumors (Supplementary Fig. S6). Whereas Mdr2-heterozygous mice preserved the typical periportal pattern of E-cadherin expression (Supplementary Fig. S6, *top row*; ref. 31), in nontumorous liver tissues of Mdr2-KO mice, E-cadherin was highly expressed in zones 1 and 2, and sometimes even in zone 3 (Supplementary Fig. S6, *middle row*). In tumors, however, its expression pattern was more heterogeneous: mostly decreased (Supplementary Fig. S6, *bottom row*) but well expressed in 5 of 16 tested tumors, similarly to human HCCs (21). Overall, there was no correlation between E-cadherin and β -catenin levels and localization.

In human cancer, an oncogenic alternatively spliced isoform of cyclin D1 was identified (32, 33). In the sequence of the intron 4 of the murine *cyclin D1* gene, we found a translation termination signal followed by a polyadenylate signal, similar to the human *cyclin D1* gene. However, we could not detect an alternatively spliced cyclin D1 isoform in either tumorous or nontumorous liver tissues of Mdr2-KO mice using RT-PCR with primers flanking the region of the suggested alternative splicing (not shown).

Discussion

Gene expression profiling of liver tissue samples of aged Mdr2-KO mice revealed many features that this HCC model

shares with previously published human and mouse HCC data. About 20% of genes differentially expressed in liver tumors of Mdr2-KO mice were also reported to be coordinately differentially expressed in human HCCs (Supplementary Table S1). The genes down-regulated in tumors were enriched with liver-specific genes, whereas genes up-regulated in tumors were enriched with cell cycle-related genes (especially, the genes specific for advanced mitotic stages), similarly with published human HCC data (13, 34). Remarkably, many tumor suppressor genes were down-regulated in three or more of the six tumors that were subjected to the whole genome expression profiling (compared with their matched nontumorous tissues). Real-time RT-PCR analysis of the expression of seven tumor suppressor genes in an expanded tumor set showed down-regulation of at least two tumor suppressors in 10 of the 16 tested tumors. Transcripts of genes *Cdh1*, *Dleu2*, *Plag1*, and *Rbl2* were down-regulated each in at least 6 tumors (Table 1). These data emphasize the critical importance of down-regulation of multiple tumor suppressor genes for the switch from nontumorous to tumorous liver tissues.

We analyzed p53 and β -catenin signaling pathways, which are frequently deregulated in HCC. No consistent pattern of differential regulation of p53 transcriptional targets was revealed in Mdr2-KO tumors. Although several genes that were previously shown to correlate with p53 immunostaining in human HCC (13) were also coordinately differentially regulated between tumor samples and heterozygotes in some Mdr2-KO tumor samples, p53 accumulation in Mdr2-KO tumors could not be detected by immunohistochemistry. However, p53 activity can be decreased not only due to mutations in the *p53* gene but also due to decreased stability of the p53 protein or interference from other proteins with its function. Thus, it was recently shown that the PTTG1 protein is frequently overexpressed in human HCC and interferes with the ability of p53 to induce apoptosis (35). In the Mdr2-KO microarray data set, the PTTG1 transcript was overexpressed >2-fold in five of the six tested liver tumors (Supplementary Table S1). Further studies are required to reveal the role of the p53 pathway in Mdr2-KO-induced hepatocarcinogenesis. We observed that most transcriptional markers of β -catenin activation were down-regulated in the majority of Mdr2-KO tumor samples. Immunohistochemical analysis revealed no cytoplasmic or nuclear β -catenin staining, as well as decreased membranous staining, in all 16 tested Mdr2-KO liver tumor samples. Nontumorous liver regions of the Mdr2-KO mice were characterized by strongly expanded expression pattern of membranous E-cadherin, which is strictly periportal in normal liver (31). Such expression pattern makes it tempting to speculate that the overexpressed E-cadherin titrates β -catenin at the plasma membrane, thus decreasing its cytoplasmic and nuclear pools. However, no correlation was found between loss of E-cadherin expression and nuclear accumulation of β -catenin either in human HCCs (21) or in other murine HCC models (36). Similarly, in liver tumors of Mdr2-KO mice, there was no correlation between E-cadherin expression level and cytoplasmic or nuclear β -catenin level.

Recently, it was shown that human and murine HCC samples could be divided into two groups that are characterized by either β -catenin activation or genomic instability (37). Based

on the genome positions of differentially expressed genes, we suggested the presence of a prolonged deletion on chromosome 8 in three of the six tested tumor samples. Deletions in chromosome 8 had already been described in mouse HCC models (38). The presumed deletion in murine chromosome 8 is syntenic to human chromosomal regions, which are frequently deleted in human HCC and contain several tumor suppressor genes. We confirmed deletion of the chromosomal region containing the *Cdh1* gene, which encodes E-cadherin, in all three presumed liver tumor samples by semiquantitative PCR. One of the possible candidates connecting the escape from mitotic arrest with chromosomal instability is the *Ubd* (Fat10) gene, which was highly up-regulated in all nontumorous and in most tumorous Mdr2-KO liver samples (Table 1 and Supplementary Tables S2 and S3). Up-regulation of the *Ubd* expression was reported in human HCC (39) but not in previously published murine HCC models. *Ubd* was shown to bind a spindle checkpoint protein, Mad211 (which was also up-regulated in Mdr2-KO tumor samples at mRNA level), at the time of mitosis, resulting in increased mitotic nondisjunction and chromosomal instability (30).

We found that genes *Gnmt*, *Ahcy*, and *Cbs* encoding three subsequent steps in catabolism of *S*-adenosylmethionine were all down-regulated in the six Mdr2-KO tumors analyzed by microarrays (Supplementary Table S1). In most of these tumors, the balance between the two forms of the methionine adenosyltransferase enzyme, which synthesizes *S*-adenosylmethionine, was disturbed: Mat1a, specific for adult liver, was down-regulated, whereas Mat2a, usually present in fetal liver, was up-regulated (data not shown). Similar changes in expression of these genes were found in human HCC cases (25, 40). Remarkably, genes *Mat1a* and *Ahcy* were also down-regulated in the livers of Mdr2-KO mice late in the precancerous stage, at 12 month of age (~2-fold in comparison with age-matched Mdr2-heterozygotes). Such disturbances in the metabolism of *S*-adenosylmethionine, a universal donor of methyl groups, may cause changes in the methylation pattern of DNA and histones affecting expression pattern of multiple genes (41).

It was previously shown that based on gene expression profiles, mouse HCC models may be divided into two groups: more similar and less similar to human HCC cases (1). Using the cross-platform and cross-species analyses, we showed that (a) the Mdr2-KO model coclusterizes with mouse HCC models that are more similar to human HCCs, and (b) most Mdr2-KO liver samples were more similar to the better-survival human HCC samples and better-survival-like mouse models (1). Among the existing murine HCC models, the Mdr2-KO mice are most similar to the E2F1-transgenic model. However, the common differentially expressed genes of Mdr2-KO and E2F1-transgenic mice were not enriched with E2F1 transcriptional targets. Both Mdr2-KO and E2F1-transgenic mice are characterized by progressive steatosis. In E2F1-transgenic mice, the transcription factor Srebp1 (Srebf1) was recently identified as a candidate responsible for induction of lipogenic enzymes (42). However, most analyzed liver tumors of Mdr2-KO mice did not show a consistent pattern of up-regulation of Srebp1 target genes, as was the case in tumors of E2F1-transgenic mice. Despite the difference in molecular mechanisms that determine the hepatocarcinogenesis in these two HCC models, they both

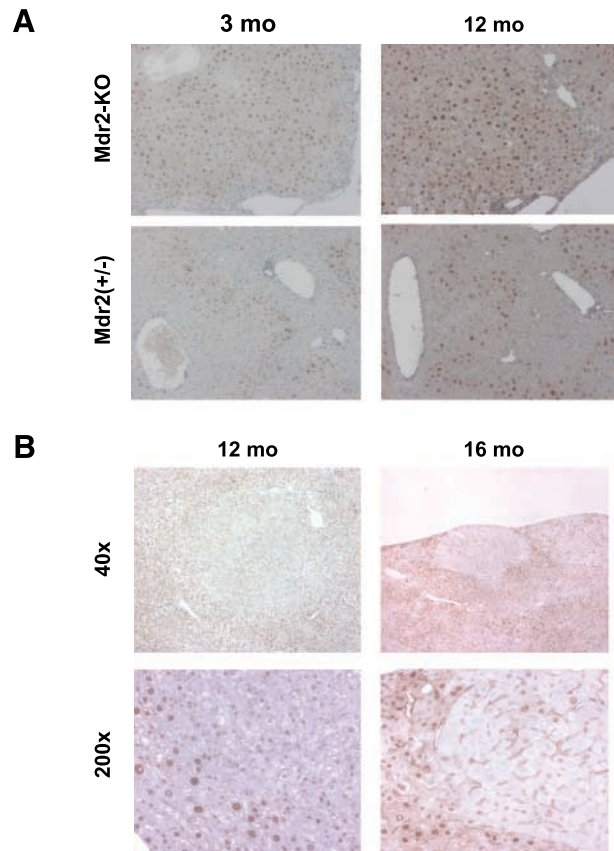
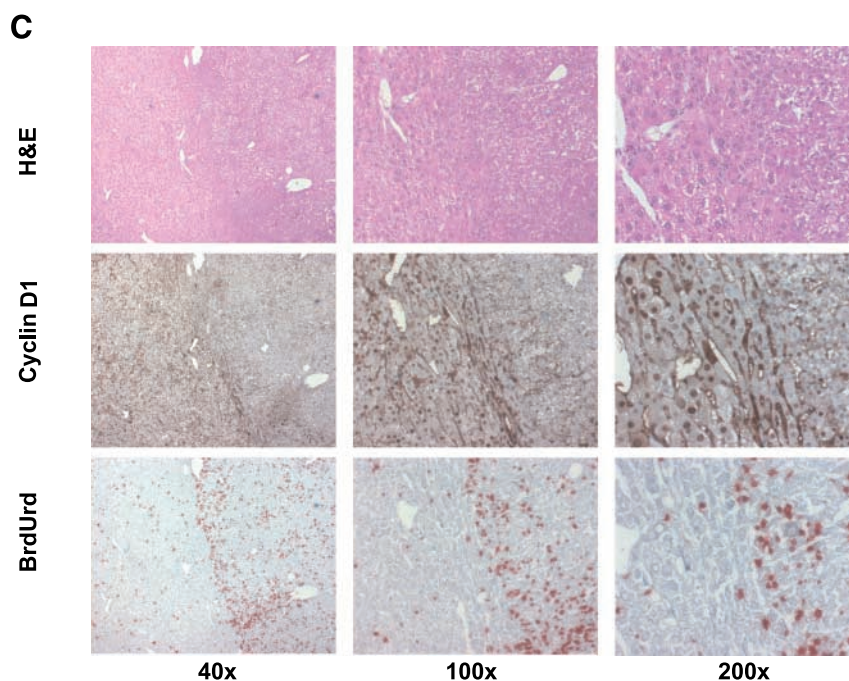


FIGURE 5. Nuclear level of cyclin D1 in hepatocytes of Mdr2-KO mice revealed by immunostaining. **A.** Increased nuclear level of cyclin D1 in Mdr2-KO mice (top row) compared with control heterozygotes (bottom row) both at age 3 mo (left column) and 12 mo (right column). Magnification, $\times 100$. **B.** Decrease of nuclear cyclin D1 level in hepatocytes of dysplastic nodules in Mdr2-KO mice at age 12 mo (left column) and 16 mo (right column). Magnification, $\times 40$ (top row) and $\times 200$ (bottom row).

show that liver steatosis is an important risk factor for liver cancer, similarly to what is known for human HCC (43).

We have recently shown that in the livers of Mdr2-KO mice, cyclin D1, a known oncogene, is overexpressed both at the mRNA and protein levels in the early and late precancerous stages (7). In the current study, we show that at the cancerous stage of liver disease, the nuclear level of cyclin D1 is increased in dysplastic hepatocytes that do not form discrete nodules but is decreased in most dysplastic nodules, especially in well-differentiated HCC. This expression pattern is independent of animal age (mice at ages 12, 14, 16, and 18 months were tested), which raises a question about the role of cyclin D1 at different stages of hepatocarcinogenesis in Mdr2-KO mice. Cyclin D1 is overexpressed at relatively early stages of different human tumors; in many cancers including HCC, its overexpression is associated with poor prognosis (44). In human HCC, the cyclin D1 level compared with surrounding nontumorous tissue correlated with tumor grade: mostly not overexpressed in well-differentiated HCC and progressively up-regulated in moderately and poorly differentiated HCC (45-47). Ultrasonography and subsequent immunohistochemical analyses of small human HCC nodules showed that



D

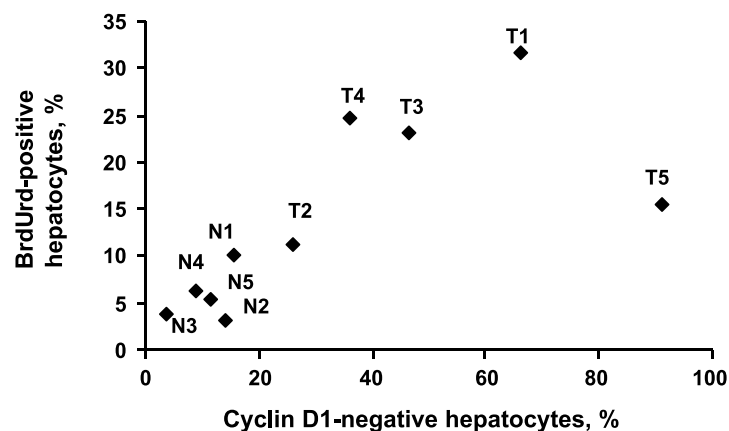


FIGURE 5 *Continued.* **C.** Increased BrdUrd inclusion and decreased nuclear cyclin D1 level in hepatocytes of a typical HCC nodule in a 16-mo-old Mdr2-KO mouse. Top row, H&E staining; middle row, cyclin D1 staining; bottom row, BrdUrd staining. Magnification, $\times 40$, $\times 100$, and $\times 200$ (left to right). **D.** Graph showing a direct correlation between the numbers of BrdUrd-positive and cyclin D1-negative hepatocyte nuclei. Pictures of the typical tumorous and their matched nontumorous regions of five livers from five 16-mo-old Mdr2-KO mice were taken at the same magnification ($\times 100$), and the percent of BrdUrd-positive and cyclin D1-negative hepatocytes was determined for each image on a computer (an average of 364 hepatocytes were counted per each image).

overexpression of cyclin D1 protein was found in only 5% of hyperechoic HCCs but in 38% of hypoechoic HCCs (mainly in moderately differentiated tumors; ref. 48). Down-regulation of cyclin D1 in some human HCC types has also been reported (34, 49, 50). Thus, down-regulation of nuclear cyclin D1 level in dysplastic nodules and in well-differentiated HCC in the livers of Mdr2-KO mice modulates its expression in some subgroups of human HCC, particularly in hyperechoic liver tumors, which are predominantly steatotic (48), as well as in many liver tumors of Mdr2-KO mice. What could be the role of this down-regulation in hepatocarcinogenesis? High levels of cyclin D1 in the cell nucleus during the S phase inhibit DNA synthesis; efficient cell proliferation requires glycogen synthase kinase 3 β -dependent phosphorylation of cyclin D1 following its export from the nucleus and subsequent degradation (51). However, the oncogenic alternatively spliced isoform of cyclin D1 lacks the phosphorylation site and remains nuclear (32),

showing that at some stage, cancer cells can overcome the inhibition of DNA synthesis by cyclin D1. Remarkably, it was recently shown that in human esophageal adenocarcinoma, the appearance of this alternatively spliced cyclin D1 isoform was associated with increased genomic instability (52). Previously, it was shown that cyclin D1 overexpression induces centrosome and mitotic spindle abnormalities, as well as aneuploidy in murine hepatocytes *in vivo* and in human breast epithelial cells *in vitro* (53). These findings reveal another potential oncogenic mechanism of prolonged nuclear accumulation of cyclin D1, which takes place in hepatocytes of Mdr2-KO mice.

We hypothesize that cyclin D1 plays different roles at different stages of hepatocarcinogenesis in Mdr2-KO mice. At the precancerous stage, overexpression of cyclin D1 in hepatocyte nuclei engenders a tumor suppressor activity by inhibiting DNA replication in most hepatocytes. Simultaneously, it may

act as an oncogene by inducing aneuploidy in some hepatocytes. The above-mentioned overexpression of the *Ubd* gene should induce aneuploidy as well. In dysplastic nodules and well-differentiated HCC, some mechanism (e.g., down-regulation of the retinoblastoma protein; ref. 54) may cause degradation of the cyclin D1 protein, thus allowing uncontrolled hepatocyte proliferation. At the later stages of moderately and poorly differentiated HCC, tumor cells may acquire an ability to bypass the inhibitory effect of cyclin D1 on DNA synthesis. At these stages, cyclin D1 is frequently overexpressed and acts as an oncogene, stimulating increased cell proliferation. Indeed, whereas most tested liver tumors in Mdr2-KO mice were well differentiated, some of them contained foci of less differentiated, “primitive” hepatocytes, which had strong nuclear cyclin D1 staining (data not shown).

Expression of cyclin D1 is regulated by multiple factors both at mRNA and protein levels (Fig. 6). Both in human and mouse HCC, activation and/or mutations of β -catenin are significantly associated with cyclin D1 overexpression. Analysis of β -catenin transcriptional targets revealed absence of activation of the classic Wnt-pathway in most HCC tumors of Mdr2-KO mice. Both in tumorous and nontumorous liver tissues, levels of cyclin D1 mRNA did not correlate with expression patterns of β -catenin targets, and nuclear level of cyclin D1 protein in hepatocytes did not correlate with nuclear or cytoplasmic level of β -catenin. Thus, in the Mdr2-KO liver, cyclin D1 is up-regulated not due to activation of β -catenin. Further studies are required to reveal the factors that regulate cyclin D1 expression in Mdr2-KO hepatocytes and the role of cyclin D1 in Mdr2-KO-induced hepatocarcinogenesis.

In conclusion, we show that the Mdr2-KO mouse may be used as a model for human HCCs that are characterized by the absence of β -catenin activation, by low nuclear cyclin D1 levels in tumor hepatocytes, and by down-regulation of multiple

tumor suppressor genes. The role of processes such as inflammation and steatosis in hepatocarcinogenesis and of HCC-associated regulatory proteins such as nuclear factor κ B (6), cyclin D1, E-cadherin, Ubd and proteins, which regulate methylation, can be studied in this HCC model.

Materials and Methods

Animal Experiments

Founders of the FVB.129P2-Abcb4^{tm1Bor} (Mdr2-KO; old name FVB.129P2-Pgy24^{tm1Bor}) and the wild-type FVB/NJ mice were purchased from The Jackson Laboratory. Colonies of both strains were maintained under specific pathogen-free conditions at the Animal Facility of The Hebrew University Medical School. The F₁ hybrids produced by breeding of an FVB.129P2-Abcb4^{tm1Bor} male and an FVB/NJ female were used as age-matched controls. Harvesting of mouse liver tissues and blood analysis for levels of liver enzymes were done as described previously (7). BrdUrd (100 mg/kg; Sigma) was injected i.p. twice: 4 and 2 h before liver resection. All animals received humane care and were kept in a specific pathogen-free facility according to the guidelines established by the U.S. National Academy of Sciences and published by the NIH.

Gene Expression Profiling

Total RNA was isolated from frozen liver tissues with Trizol reagent (Invitrogen) as described by the manufacturer and subjected to genome-scale gene expression profiling using Mouse Genome Array 430A (Affymetrix, Inc.). The gene expression values were extracted using the MAS 5.0 software and, after thresholding and filtering procedures, were submitted to fold change and cluster analyses (see Supplementary Methods for details). The expression data are accessible on the GEO site, represented according to the MIAME requirements.

Comparison with Published Data Sets

The Affymetrix expression data for the Mdr2-KO model were presented as data on gene differential expression (in the format of the output of two-color spotted arrays) by calculating the log ratio of the expression values in Mdr2-KO samples to the average of Mdr2-KO heterozygous controls. The joint data sets containing our data and the data of other research groups were created and analyzed as described in Supplementary Methods.

Chromosomal Analysis

Smoothed fold change values have been calculated for all annotated genes that were relevant for position-specific fold change analysis and plotted against their chromosomal positions (see Supplementary Methods for details).

Real-time RT-PCR

Reverse transcription of total RNA was done using the Moloney murine leukemia virus reverse transcriptase enzyme and random hexamer primers from Promega. Real-time PCR was run in triplicates using the TaqMan Universal PCR Master Mix, primers and probe sets, and the ABI PRISM 7700 Sequence Detector system from Applied Biosystems. Threshold cycle numbers (*C_t*) were determined with Sequence Detector Software (version 1.6; Applied Biosystems) and transformed

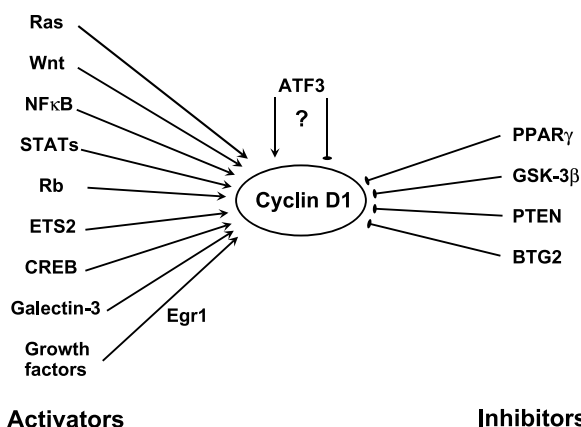


FIGURE 6. Positive and negative regulations of the cyclin D1 expression level. The scheme shows the main activators and inhibitors of cyclin D1 expression (both at mRNA and protein levels). For activating transcription factor 3 (*ATF3*), both activatory and inhibitory effects on cyclin D1 expression were reported. NF κ B, nuclear factor κ B; STATs, signal transducers and activators of transcription; ETS2, erythroblastosis virus oncogene homologue 2; CREB, cyclic AMP-responsive element binding protein; PPAR γ , peroxisome proliferator-activated receptor γ ; GSK-3 β , glycogen synthase kinase 3 β ; PTEN, phosphatase and tensin homologue; BTG2, B-cell translocation gene 2; Rb, retinoblastoma; Egr1, early growth response 1.

using the ΔC_t method as described by the manufacturer. The relative quantification values for each gene were normalized against the endogenous “housekeeping” gene *Arl6ip1*, which was one of the most uniformly expressed genes in all RNA samples subjected to global gene expression profiling.

Immunohistochemistry

Immunostaining was done on 4- μ m-thick formalin-fixed paraffin-embedded liver tissue sections by standard procedures. Antigen retrieval was done with citrate buffer (pH 6.0; β -catenin, p53, and BrdUrd), Tris-EGTA buffer (pH 9.0; E-cadherin), or glycine buffer (pH 9.0; cyclin D1) in a microwave by boiling (BrdUrd) or using a pressure cooker (cyclin D1, β -catenin, E-cadherin, and p53). Primary antibodies were cyclin D1 (RMA003; Diagnostic Biosystems), β -catenin (clone 14; BD Biosciences), E-cadherin (24E10; Cell Signaling Technology, Inc.), p53 (CM5p; Vision Biosystems/Novocastra), and BrdUrd (Mo744; DAKO). Secondary antibodies were from DAKO or Zymed. Staining was developed with diaminobenzidine using a kit from Zymed (cyclin D1, E-cadherin, p53, and β -catenin) or with 3-amino-9-ethylcarbazole (BrdUrd) using a kit from DAKO.

Acknowledgments

We thank our colleagues from Hadassah-Hebrew University Medical Center: Prof. Leslie Ann Mitchell and Dr. Amnon Peled (Goldyne Savad Institute of Gene Therapy) for useful discussions; Dr. Eli Pikarsky (Department of Pathology) for his help in immunohistochemistry techniques and sharing unpublished data; Prof. Yinon Ben-Neriah (The Lautenberg Center for Immunology) for providing antibodies, protocol, and a positive control for p53 immunostaining; Ariel Israel, Carol Levy, and Mery Clausen (Goldyne Savad Institute of Gene Therapy) for their assistance in bioinformatics, work with mice, and manuscript preparation, respectively.

References

- Lee JS, Chu IS, Mikaelian A, et al. Application of comparative functional genomics to identify best-fit mouse models to study human cancer. *Nat Genet* 2004;36:1306–11.
- Lee JS, Grisham JW, Thorgeirsson SS. Comparative functional genomics for identifying models of human cancer. *Carcinogenesis* 2005;26:1013–20.
- Mauad TH, van Nieuwkerk CM, Dingemans KP, et al. Mice with homozygous disruption of the *mdr2* P-glycoprotein gene. A novel animal model for studies of nonsuppurative inflammatory cholangitis and hepatocarcinogenesis. *Am J Pathol* 1994;145:1237–45.
- Fickert P, Fuchsbieler A, Wagner M, et al. Regurgitation of bile acids from leaky bile ducts causes sclerosing cholangitis in *Mdr2* (*Abcb4*) knockout mice. *Gastroenterology* 2004;127:261–74.
- De Vree JM, Ottenhoff R, Bosma PJ, Smith AJ, Aten J, Oude Elferink RP. Correction of liver disease by hepatocyte transplantation in a mouse model of progressive familial intrahepatic cholestasis. *Gastroenterology* 2000;119:1720–30.
- Pikarsky E, Porat RM, Stein I, et al. NF- κ B functions as a tumour promoter in inflammation-associated cancer. *Nature* 2004;431:461–6.
- Katzenellenbogen M, Pappo O, Barash H, et al. Multiple adaptive mechanisms to chronic liver disease revealed at early stages of liver carcinogenesis in the *Mdr2*-knockout mice. *Cancer Res* 2006;66:4001–10.
- Lee JS, Chu IS, Heo J, et al. Classification and prediction of survival in hepatocellular carcinoma by gene expression profiling. *Hepatology* 2004;40:667–76.
- Blatt M, Wiseman S, Domany E. Superparamagnetic clustering of data. *Phys Rev Lett* 1996;76:3251–4.
- Getz G, Levine E, Domany E. Coupled two-way clustering analysis of gene microarray data. *Proc Natl Acad Sci U S A* 2000;97:12079–84.
- Cadore A, Ovejero C, Terris B, et al. New targets of β -catenin signaling in the liver are involved in the glutamine metabolism. *Oncogene* 2002;21:8293–301.
- Sekine S, Lan BY, Bedolli M, Feng S, Hebrok M. Liver-specific loss of β -catenin blocks glutamine synthesis pathway activity and cytochrome p450 expression in mice. *Hepatology* 2006;43:817–25.
- Chen X, Cheung ST, So S, et al. Gene expression patterns in human liver cancers. *Mol Biol Cell* 2002;13:1929–39.
- Buendia MA. Genetics of hepatocellular carcinoma. *Semin Cancer Biol* 2000;10:185–200.
- Crawley JJ, Furge KA. Identification of frequent cytogenetic aberrations in hepatocellular carcinoma using gene-expression microarray data. *Genome Biol* 2002;3:RESEARCH0075.
- Jou YS, Lee CS, Chang YH, et al. Clustering of minimal deleted regions reveals distinct genetic pathways of human hepatocellular carcinoma. *Cancer Res* 2004;64:3030–6.
- Fujiwara Y, Ohata H, Emi M, et al. A 3-Mb physical map of the chromosome region 8p21.3-p22, including a 600-kb region commonly deleted in human hepatocellular carcinoma, colorectal cancer, and non-small cell lung cancer. *Genes Chromosomes Cancer* 1994;10:7–14.
- Fujiwara Y, Ohata H, Kuroki T, et al. Isolation of a candidate tumor suppressor gene on chromosome 8p21.3-p22 that is homologous to an extracellular domain of the PDGF receptor β gene. *Oncogene* 1995;10:891–5.
- Xu Z, Liang L, Wang H, Li T, Zhao M. HCRP1, a novel gene that is down-regulated in hepatocellular carcinoma, encodes a growth-inhibitory protein. *Biochem Biophys Res Commun* 2003;311:1057–66.
- Park EY, Cho IJ, Kim SG. Transactivation of the PPAR-responsive enhancer module in chemopreventive glutathione S-transferase gene by the peroxisome proliferator-activated receptor- γ and retinoid X receptor heterodimer. *Cancer Res* 2004;64:3701–13.
- Wei Y, Van Nhieu JT, Prigent S, Srivatanakul P, Tiollais P, Buendia MA. Altered expression of E-cadherin in hepatocellular carcinoma: correlations with genetic alterations, β -catenin expression, and clinical features. *Hepatology* 2002;36:692–701.
- Huynh H. Overexpression of tumour suppressor retinoblastoma 2 protein (pRb2/p130) in hepatocellular carcinoma. *Carcinogenesis* 2004;25:1485–94.
- Kochetkova M, McKenzie OL, Bais AJ, et al. CBFA2T3 (MTG16) is a putative breast tumor suppressor gene from the breast cancer loss of heterozygosity region at 16q24.3. *Cancer Res* 2002;62:4599–604.
- Tsafirir D, Tsafirir I, Ein-Dor L, Zuk O, Notterman DA, Domany E. Sorting points into neighborhoods (SPIN): data analysis and visualization by ordering distance matrices. *Bioinformatics* 2005;21:2301–8.
- Avila MA, Berasain C, Torres L, et al. Reduced mRNA abundance of the main enzymes involved in methionine metabolism in human liver cirrhosis and hepatocellular carcinoma. *J Hepatol* 2000;33:907–14.
- Eferl R, Ricci R, Kenner L, et al. Liver tumor development: c-Jun antagonizes the proapoptotic activity of p53. *Cell* 2003;112:181–92.
- Kondoh N, Hada A, Ryo A, et al. Activation of Galectin-1 gene in human hepatocellular carcinoma involves methylation-sensitive complex formations at the transcriptional upstream and downstream elements. *Int J Oncol* 2003;23:1575–83.
- Neo SY, Leow CK, Vega VB, et al. Identification of discriminators of hepatoma by gene expression profiling using a minimal data set approach. *Hepatology* 2004;39:944–53.
- Iizuka N, Oka M, Yamada-Okabe H, et al. Self-organizing-map-based molecular signature representing the development of hepatocellular carcinoma. *FEBS Lett* 2005;579:1089–100.
- Ren J, Kan A, Leong SH, et al. FAT10 plays a role in the regulation of chromosomal stability. *J Biol Chem* 2006;281:11413–21.
- Hailfinger S, Jaworski M, Braeuning A, Buchmann A, Schwarz M. Zonal gene expression in murine liver: lessons from tumors. *Hepatology* 2006;43:407–14.
- Lu F, Gladden AB, Diehl JA. An alternatively spliced cyclin D1 isoform, cyclin D1b, is a nuclear oncogene. *Cancer Res* 2003;63:7056–61.
- Knudsen KE, Diehl JA, Haiman CA, Knudsen ES. Cyclin D1: polymorphism, aberrant splicing and cancer risk. *Oncogene* 2006;25:1620–8.
- Okabe H, Satoh S, Kato T, et al. Genome-wide analysis of gene expression in human hepatocellular carcinomas using cDNA microarray: identification of genes involved in viral carcinogenesis and tumor progression. *Cancer Res* 2001;61:2129–37.
- Jung CR, Yoo J, Jang YJ, et al. Adenovirus-mediated transfer of siRNA against PTTG1 inhibits liver cancer cell growth *in vitro* and *in vivo*. *Hepatology* 2006;43:1042–52.
- Calvisi DF, Ladu S, Conner EA, Factor VM, Thorgeirsson SS. Disregulation of E-cadherin in transgenic mouse models of liver cancer. *Lab Invest* 2004;84:1137–47.

37. Calvisi DF, Factor VM, Ladu S, Conner EA, Thorgeirsson SS. Disruption of β -catenin pathway or genomic instability define two distinct categories of liver cancer in transgenic mice. *Gastroenterology* 2004;126:1374–86.
38. Davis LM, Caspary WJ, Sakallah SA, et al. Loss of heterozygosity in spontaneous and chemically induced tumors of the B6C3F1 mouse. *Carcinogenesis* 1994;15:1637–45.
39. Lee CG, Ren J, Cheong IS, et al. Expression of the FAT10 gene is highly up-regulated in hepatocellular carcinoma and other gastrointestinal and gynecological cancers. *Oncogene* 2003;22:2592–603.
40. Yang H, Huang ZZ, Zeng Z, Chen C, Selby RR, Lu SC. Role of promoter methylation in increased methionine adenosyltransferase 2A expression in human liver cancer. *Am J Physiol Gastrointest Liver Physiol* 2001;280:G184–90.
41. Avila MA, Garcia-Trevijano ER, Martinez-Chantar ML, et al. S-Adenosyl-methionine revisited: its essential role in the regulation of liver function. *Alcohol* 2002;27:163–7.
42. Coulouarn C, Gomez-Quiroz LE, Lee JS, et al. Oncogene-specific gene expression signatures at preneoplastic stage in mice define distinct mechanisms of hepatocarcinogenesis. *Hepatology* 2006;44:1003–11.
43. Kojiro M, Nakashima O. Histopathologic evaluation of hepatocellular carcinoma with special reference to small early stage tumors. *Semin Liver Dis* 1999;19:287–96.
44. Nishida N, Fukuda Y, Komeda T, et al. Amplification and overexpression of the cyclin D1 gene in aggressive human hepatocellular carcinoma. *Cancer Res* 1994;54:3107–10.
45. Masaki T, Shiratori Y, Rengifo W, et al. Cyclins and cyclin-dependent kinases: comparative study of hepatocellular carcinoma versus cirrhosis. *Hepatology* 2003;37:534–43.
46. Ito Y, Matsuura N, Sakon M, et al. Expression and prognostic roles of the G1-S modulators in hepatocellular carcinoma: p27 independently predicts the recurrence. *Hepatology* 1999;30:90–9.
47. Ramos E, Llado L, Serrano T, et al. Utility of cell-cycle modulators to predict vascular invasion and recurrence after surgical treatment of hepatocellular carcinoma. *Transplantation* 2006;82:753–8.
48. Yamagata M, Masaki T, Okudaira T, et al. Small hyperechoic nodules in chronic liver diseases include hepatocellular carcinomas with low cyclin D1 and Ki-67 expression. *Hepatology* 1999;29:1722–9.
49. Peng SY, Chou SP, Hsu HC. Association of down-regulation of cyclin D1 and of overexpression of cyclin E with p53 mutation, high tumor grade and poor prognosis in hepatocellular carcinoma. *J Hepatol* 1998;29:281–9.
50. Jung YJ, Lee KH, Choi DW, et al. Reciprocal expressions of cyclin E and cyclin D1 in hepatocellular carcinoma. *Cancer Lett* 2001;168:57–63.
51. Guo Y, Yang K, Harwalkar J, et al. Phosphorylation of cyclin D1 at Thr 286 during S phase leads to its proteasomal degradation and allows efficient DNA synthesis. *Oncogene* 2005;24:2599–612.
52. Izzo JG, Wu TT, Wu X, et al. Cyclin D1 guanine/adenine 870 polymorphism with altered protein expression is associated with genomic instability and aggressive clinical biology of esophageal adenocarcinoma. *J Clin Oncol* 2007;25:698–707.
53. Nelsen CJ, Kuriyama R, Hirsch B, et al. Short term cyclin D1 overexpression induces centrosome amplification, mitotic spindle abnormalities, and aneuploidy. *J Biol Chem* 2005;280:768–76.
54. Muller H, Lukas J, Schneider A, et al. Cyclin D1 expression is regulated by the retinoblastoma protein. *Proc Natl Acad Sci U S A* 1994;91:2945–9.